REPORT DOCUMENTATION PAGE

Public reporting burden for this collection of information is estimated to average 1 hour per response, including the time for reviewing instructions, searching existing data sources, gathering and maintaining the data needed, and completing and reviewing the collection of information. Send comments regarding this burden estimate or any other aspect of this collection of information, including suggestions for reducing this burden, to Washington Headquarters Services, Directorate for Information Operations and Reports, 1215 Jefferson Davis Highway, Suite 1204, Arlington, VA 22202-4302, and to the Office of Management and Budget, Paperwork Reduction Project (0704-0188), Washington, DC 20503.

1. AGENCY USE ONLY (Leave blank)	2. REPORT DATE 23 May 1998	3. REPORT TYPE AND DATES COVERED Technical

4. TITLE AND SUBTITLE
Reactions of $H_3Al \cdot NMe_3$ with $E(SiMe_3)_3$ (E = P, As). Structural Characterization of the Trimer $[H_2AlP(SiMe_3)_2]_3$ and Base-Stabilized Adduct $[H_2AlAs(SiMe_3)_2] \cdot NMe_3$, and Their Thermal Decomposition Toward Nanocrystalline AlP and AlAs, Respectively.

5. FUNDING NUMBERS
N00014-95-1-0194
R&T Project 3135008---16.

6. AUTHOR(S)
J. F. Janik, R. L. Wells, P. S. White

Dr. Harold E. Guard

7. PERFORMING ORGANIZATION NAME(S) AND ADDRESS(ES)
Department of Chemistry
Duke University,
Durham, NC 27708-0346

8. PERFORMING ORGANIZATION REPORT NUMBER
Technical Report
No. DU/DC/TR-76

9. SPONSORING / MONITORING AGENCY NAME(S) AND ADDRESS(ES)
Office of Naval Research
300 North Quincy Street
Arlington, VA 22217-5000

10. SPONSORING / MONITORING AGENCY REPORT NUMBER

11. SUPPLEMENTARY NOTES
Accepted for publication in the *Inorganic Chemistry*

19980601 079

12a. DISTRIBUTION / AVAILABILITY STATEMENT
Approved for Public Release
Distribution Unlimited

12b. DISTRIBUTION CODE

13. ABSTRACT (Maximum 200 words)

Dehydrosilylation reactions in diethyl ether between $H_3Al \cdot NMe_3$ and $E(SiMe_3)_3$ afforded for E = P a high yield of the trimer $[H_2AlP(SiMe_3)_2]_3$ (**1**) while for E = As a monomeric base-stabilized adduct $[H_2AlAs(SiMe_3)_2] \cdot NMe_3$ (**2**) as well as its degradation solid product were obtained. No reaction occurred for E = N. The single-crystal X-ray structure determination for **1** yielded a planar six-membered ring of alternating four-coordinated Al and P centers. The structural solution for **2** revealed the monomeric unit $[H_2AlAs(SiMe_3)_2]$ stabilized by coordination of NMe_3 at the Al-site. Pyrolysis of **1** at 450 °C promoted further dehydrosilylation and yielded a product which by XRD spectroscopy showed the onset of AlP crystallinity while at 950 °C afforded nanocrystalline AlP with 5 nm average particle size. Pyrolysis of **2** at 450 °C resulted in the formation of nanocrystalline AlAs with 2 nm average particle size. Under applied pyrolysis conditions for **1** and **2**, the target elimination-condensation pathway *via* dehydrosilylation was accompanied by other decomposition side reactions and retention of some contaminant residues.

14. SUBJECT TERMS
aluminum arsenide aluminumphosphide, nanocrystalline, dehydrosilylation

15. NUMBER OF PAGES
25

16. PRICE CODE

17. SECURITY CLASSIFICATION OF REPORT Unclassified	18. SECURITY CLASSIFICATION OF THIS PAGE Unclassified	19. SECURITY CLASSIFICATION OF ABSTRACT Unclassified	20. LIMITATION OF ABSTRACT Unlimited

OFFICE OF NAVAL RESEARCH

Reactions of H3Al•NMe3 with E(SiMe3)3 (E = P, As). StructuralCharacterization of the Trimer [H2AlP(SiMe3)2]3 and Base-Stabilized Adduct [H2AlAs(SiMe3)2]•NMe3, and Their Thermal Decomposition Toward Nanocrystalline AlP and AlAs, Respectively.

Jerzy F. Janik, Richard L. Wells
Department of Chemistry, Paul M. Gross Chemical Laboratory, Duke University
Durham, NC 27708-0346

Peter S. White
Department of Chemistry, University of North Carolina at Chapel Hill,
Chapel Hill, NC 27514

Duke University
Department of Chemistry,
P. M. Gross Chemical Laboratory
Box 90346
Durham, NC 27708-0346

23 May 1998

Reactions of H$_3$Al·NMe$_3$ with E(SiMe$_3$)$_3$ (E = P, As). Structural Characterization of the Trimer [H$_2$AlP(SiMe$_3$)$_2$]$_3$ and Base-Stabilized Adduct [H$_2$AlAs(SiMe$_3$)$_2$]·NMe$_3$, and Their Thermal Decomposition Toward Nanocrystalline AlP and AlAs, Respectively.

Jerzy F. Janik,[‡] Richard L. Wells[*]

Department of Chemistry, Paul M. Gross Chemical Laboratory, Duke University

Durham, NC 27708-0346

Peter S. White

Department of Chemistry, University of North Carolina at Chapel Hill,

Chapel Hill, NC 27514

Abstract: Dehydrosilylation reactions in diethyl ether between H$_3$Al·NMe$_3$ and E(SiMe$_3$)$_3$ afforded for E = P a high yield of the trimer [H$_2$AlP(SiMe$_3$)$_2$]$_3$ (**1**) while for E = As a monomeric base-stabilized adduct [H$_2$AlAs(SiMe$_3$)$_2$]·NMe$_3$ (**2**) as well as its degradation solid product were obtained. No reaction occurred for E = N. The single-crystal X-ray structure determination for **1** yielded a planar six-membered ring of alternating four-coordinated Al and P centers. The structural solution for **2** revealed the monomeric unit [H$_2$AlAs(SiMe$_3$)$_2$] stabilized by coordination of NMe$_3$ at the Al-site. Pyrolysis of **1** at 450 °C promoted further dehydrosilylation and yielded a product which by XRD spectroscopy showed the onset of AlP crystallinity while at 950 °C afforded nanocrystalline AlP with 5 nm average particle size. Pyrolysis of **2** at 450 °C resulted in the formation of nanocrystalline AlAs with 2 nm average particle size. Under applied pyrolysis conditions for **1** and **2**, the target elimination-condensation pathway *via*

dehydrosilylation was accompanied by other decomposition side reactions and retention of some contaminant residues.

---

* To whom correspondence should be addressed.

‡ On leave from the University of Mining and Metallurgy, Krakow, Poland.

Introduction

Dehydrosilylation elimination-condensation reactions are characterized by a commonly facile evolution of volatile $HSiMe_3$ with concurrent formation of the $M(13)$–$E(15)$ bond according to the scheme: $\{R^1M(13)\} + \{E(15)R^2\} = \{M(13)-E(15)\} + HSiMe_3$; R^1, R^2 = H, $SiMe_3$ or R^1, R^2 = $SiMe_3$, H; however, only a few reports seem to have been published in this area.[1] Regarding this chemistry, we have reported on a number of occasions our studies on dehydrosilylation as a means for making 13–15 bonds and formation of potential precursors to 13–15 ceramic and semiconductor materials.[2] Thus, the reactions between $LiGaH_4$ and $E(SiMe_3)_3$ (E = P, As) afford new lithium pnictidogallates, $(Et_2O)_2Li[\mu-E(SiMe_3)_2]_2GaH_2$, featuring a planar four-membered ring in which the Li and Ga atoms are bridged by two E atoms.[2a] Similarly, the reactions of $LiAlH_4$ and $E(SiMe_3)_3$ (E = P, As) yield lithium pnictidoaluminates, $(Et_2O)_2Li[\mu-E(SiMe_3)_2]_2AlH_2$, structurally isomorphous with their gallium counterparts.[2b] The new lithium pnictidometallates may be useful starting materials for mixed-metal derivatives containing two different group 13 elements which, upon further elimination-condensation, could lead to ternary (or higher) 13–15 materials.

An extension of this chemistry to the system $H_3Ga\cdot NMe_3/E(SiMe_3)_3$ (E = P, As) has also been fruitful and resulted in the trimers $[H_2GaE(SiMe_3)_2]_3$ – the rare examples of a phosphinogallane and arsinogallane containing GaH_2, the parent gallane functionality.[2c] Prior to that, the related phosphinoborane $[H_2BP(SiMe_3)_2]_3$ was isolated from the system $H_3B\cdot THF/P(SiMe_3)_3$[1a] and phosphinogallane $(H_2GaPCy_2)_3$ was made *via* salt elimination from the combination of $H_2(Cl)Ga\cdot PCy_3$ and $LiPCy_2\cdot nTHF$, Cy = cyclohexyl.[3a] Interestingly, the structures of all three trimers containing four-coordinated group 13 and $SiMe_3$-bound group 15 atoms show significant ring flattening or planarity. They also display curious incidents of the thermal parameters for the group 13 atom being about twice the magnitude of the group 15 atom, yet both atoms occupy structurally similar positions in

the ring. This property, that could be linked to deviations from ring planarity, appears to be a specific feature in this family of compounds. That the reasons behind it are not quite obvious is illustrated by the structural solution for the sterically similar trimer [t-Bu$_2$GaPH$_2$]$_3$ which provides a planar ring core while thermal parameters for Ga and P appear to be comparable.[3b] More structural data are clearly needed to better understand these phenomena.

The cases discussed above reveal that oligomerization of the likely transient monomeric unit formed upon dehydrosilylation, [H$_2$ME(SiMe$_3$)$_2$], is favored over plausible stabilization of the monomer with the available NMe$_3$, a potent Lewis base. However, there are known cases which yield base-stabilized adducts, instead. For example, dihydrogen elimination from the combinations of H$_3$Al•NMe$_3$ or H$_2$ClAl•NMe$_3$ and HN(SiMe$_3$)$_2$, is reported to yield [H$_2$AlN(SiMe$_3$)$_2$]•NMe$_3$[4] or [H(Cl)AlN(SiMe$_3$)$_2$]•NMe$_3$,[4c] respectively. The preference of the base-stabilized adducts over oligomerization products in these cases could perhaps be linked to a mere latent basicity of the nitrogen atom in N(SiMe$_3$)$_2$, the property that could further be enhanced by steric congestion imposed by this ligand; to the best of our knowledge, there have not been reported ring structures featuring bridging N(SiMe$_3$)$_2$ groups. Other examples include salt-elimination reactions in the system LiE(Mes)$_2$/H$_2$ClAl•NMe$_3$, E = P, As, which also result in the base stabilized adducts [H$_2$AlEMes$_2$]•NMe$_3$.[5] All these cases do not provide, however, sufficient comparative data to understand the outcome of the reactions in systems containing a strong Lewis base as is the case of the convenient forms of alane and gallane, H$_3$M•NMe$_3$, M = Al, Ga.

Herein we describe reactivity in the systems H$_3$Al•NMe$_3$/E(SiMe$_3$)$_3$, E = N, P, As, and the formation and structural characterization of the trimer [H$_2$AlP(SiMe$_3$)$_2$]$_3$ (1) and monomeric base-stabilized adduct [H$_2$AlAs(SiMe$_3$)$_2$]•NMe$_3$ (2); the latter compound, if not isolated and stored at −30 °C, spontaneously decomposes to a white insoluble solid. We

conclude this report with preliminary results of the pyrolyses of **1** and **2** that yield nanocrystalline AlP and AlAs, respectively.

Experimental Section

General Techniques. All experiments were carried out using standard vacuum/Schlenk techniques.[6] Solvents were dried and distilled from Na benzophenone ketyl or Na/K alloy prior to use. $N(SiMe_3)_3$ was purchased from Aldrich and used as received. $H_3Al\cdot NMe_3$,[7] $P(SiMe_3)_3$,[8] and $As(SiMe_3)_3$[9] were prepared by the literature methods. ^1H, $^{13}C\{^1H\}$, and ^{31}P NMR spectra were acquired on a Varian Unity 400 spectrometer at 25 °C from toluene-d_8 or benzene-d_6 solutions and referenced *vs* $SiMe_4$ by generally accepted methods. Mass spectra were collected on a JEOL JMS-SX 102A spectrometer operating in the EI mode at 20 eV; the CI mode (isobutane) yielded comparable results. IR spectra of solids and gaseous pyrolysis products were acquired using KBr pellets and a gas cell, respectively, on a BOMEM Michelson MB-100 FT-IR spectrometer. A calibrated manifold was used for volume estimations of reaction gases. Elemental analyses were provided by E+R Microanalytical Laboratory, Corona, NY. Melting behavior (uncorrected) was determined with a Thomas-Hoover Uni-melt apparatus for samples flame-sealed in glass capillaries. TGA/DTA analyses were performed under an UHP nitrogen flow and 5 °C/min heating rate on a TA Instruments SDT 2960 simultaneous TGA/DTA apparatus. Single-crystal X-ray diffraction studies for **1** (223 K) and **2** (173 K) were performed at the University of North Carolina at Chapel Hill, Chapel Hill, NC, on a Siemens SMART Platform CCD system using Mo K_α radiation ($\lambda = 0.71073$ Å). All calculations were carried out with the help of NRCVAX programs;[10] the structures were solved by direct methods. XRD data for powders were collected using mineral oil coated samples on a Phillips XRD 3000 diffractometer utilizing Cu $K\alpha$ radiation; the average particle sizes of the AlP and AlAs

products were calculated using the Scherrer equation applied to the (111) diffraction lines of the cubic AlP (JCPDS file 12-470) and cubic AlAs (JCPDS file 17-915).

Reaction system $H_3Al \cdot NMe_3/P(SiMe_3)_3$ in Et_2O.

(1) Synthesis and characterization of $[H_2AlP(SiMe_3)_2]_3$ (1). A sample of freshly prepared $H_3Al \cdot NMe_3$, 0.54 g or 6.0 mmol, was dissolved in 20 mL of Et_2O and a solution of $P(SiMe_3)_3$ in 20 mL of Et_2O, 1.50 g or 6.0 mmol, was added to it at room temperature. Several minutes after addition, the mixture turned slightly milky. It was stirred at ambient conditions overnight, some white insoluble solid filtered out, and the filtrate concentrated by evacuation to a few milliliters. After 2–3 days at –30 °C, abundant colorless crystals of **1** appeared, 0.85 g or 69% yield based on eq 1 (*vide infra*); even more crystals could be recovered upon further work-up of the solution. Melting behavior: 70–150 °C, visible decomposition with massive gas evolution; above 200 °C, change of color to yellow and golden-red; no melting to 300 °C. Anal. Found (calcd) for $C_{18}H_{60}Al_3P_3Si_6$: C, 34.65 (34.92); H, 9.60 (9.77). ^1H NMR (toluene-d_8): δ 0.481, 0.485, 0.489, 0.493 (equally spaced four-line multiplet with relative intensities 80:100:100:80 and separation of 1.7 Hz, 54H; $SiMe_3$), 4.4 (6H, br; AlH_2). $^{13}C\{^1H\}$ NMR (tolune-d_8) (intensity): four-line multiplet at δ 2.44 (sh, 70), 2.47 (100), 2.49 (100), 2.52 (sh, 60); $SiMe_3$. $^{31}P\{^1H\}$ NMR (toluene-d_8): δ -273.5. MS: m/e (intensity) (ion): peak clusters around: 617 (5) ($[H_2AlP(SiMe_3)_2]_3$ – H or M – H), 588 (2) (M – 2Me), 543 (13) (M – $SiMe_3$ – 2H), 514 (7) (M – $SiMe_3$ – 2Me – H), 441 (55) (M – $P(SiMe_3)_2$), 412 (100) ($[H_2AlP(SiMe_3)_2]_2$ or M^*), 397 (9) (M^* – Me), 367 (57) (M^* – 3Me), 351 (30) (M^* – 4Me – H), 338 (100) (M^* – $SiMe_3$ – H), 323 (36) (M^* – $SiMe_3$ – Me – H), 309 (16) (M^* – $SiMe_3$ – 2Me), 293 (21) (M^* – $SiMe_3$ – 3Me – H), 279 (51) (M^* – $SiMe_3$ – 4Me), 264 (78) (M^* – $2SiMe_3$ – 2H), 249 (18) (M^* – $2SiMe_3$ – Me – 2H), 234 (18) (M^* – $2SiMe_3$ – 2Me – 2H), 205 (26) ($H_2AlP(SiMe_3)_2$ – H or M^{**} – H), 191 (M^{**} – Me), 178 (38) ($HP(SiMe_3)_2$), 174 (23) (M^{**} – 2Me – 2H), 163 (21) ($HP(SiMe_3)_2$ – Me), 160 (16) (M^{**} – 3Me – H), 73 (61)

(SiMe₃), 59 (4) (HSiMe₂). IR: ν(Al–H) 1796 cm⁻¹. Note, the NMR spectra for raw decanted crystals of 1 show also resonances for some residual P(SiMe₃)₃ as well as a set of apparently correlated signals in the ¹H NMR spectrum at δ 0.504 (that could be a part of a doublet partially buried under the major four-line multiplet) and 1.89 (s; NMe₃) which seem to correspond to the ¹³C{¹H} NMR resonances at δ 4.96 (d, $^2J_{P–C}$ = 10.7 Hz; SiMe₃) and 47.4 (s; NMe₃) in a minor byproduct.

(2) Thermal decomposition. Significant TGA weight changes commenced at 60 °C and exhibited one major weight loss to 250 °C, 55%, followed by a smaller loss to 450 °C, 3.5%; total weight loss of 58.5%. Calculated weight loss for: [H₂AlP(SiMe₃)₂]₃ = 3AlP + 6HSiMe₃, 71.9%. A sample of 1, 0.40g or 0.65 mmol, was pyrolyzed in a sublimer for two hours at 450 °C under vacuum and with the collection of volatiles. Small quantities of a colorless, oily liquid, likely P(SiMe₃)₃, distilled out onto colder parts of the set-up together with brown solid deposits which were additionally observed after completion of pyrolysis. Also, the inner surface of the sublimer was deposited with a shiny, coppertone-like solid film which could not easily be removed afterwards. The major product was a brown solid, 0.10 g or weight loss of 75%. Noncondensables (CH₄ and H₂), 0.9 mmol; condensables (HSiMe₃), 2.5 mmol; weight of volatiles, approximately 0.2 g. An XRD pattern for the brown product showed two extremely broad features at 2Θ 30° and 50° consistent with the onset of AlP crystallinity; average particle size, < 1 nm. A similar pyrolysis experiment was carried out at 950 °C without the collection of volatiles. A dark gray/black solid product was obtained whose XRD spectrum matched JCPDS file 12-470 for cubic AlP; average particle size, 5 nm. EA: Al, 28.62; P, 33.53; Si, 11.31; C, 4.69; H, 0.62; P/Al = 1.02; C/Si = 0.97. Also, the whole length of the pyrolysis tube was vapor-deposited inside with a thin and shiny, golden-like solid film.

Reaction system $H_3Al \cdot NMe_3/As(SiMe_3)_3$ in Et_2O.

(1) Synthesis and characterization of $[H_2AlAs(SiMe_3)_2] \cdot NMe_3$ (2).
Typically, a sample of freshly prepared $H_3Al \cdot NMe_3$, 0.45 g or 5.0 mmol, was dissolved in 20 mL of Et_2O and a solution of $As(SiMe_3)_3$ in 20 mL of Et_2O, 1.47 g or 5.0 mmol, was added to it at room temperature. The mixture turned milky several minutes after addition. It was stirred overnight, a relatively small quantity of the insoluble solid was filtered out, the solution concentrated by evacuation to a few milliliters, and stored at −30 °C. After 4 weeks under these conditions only some insoluble white solid precipitated. Sizable quantities of crystalline **2** were obtained by either of the two following methods. First, **2** crystallized from the original Et_2O solution that was subsequently evacuated almost entirely in the course of several hours at −30 °C. Alternatively, the ether was removed from a portion of the original mixture, the solids redissolved in toluene, and the concentrated solution stored in an opened vial at −30 °C (dry-lab freezer); such a slow evaporation of the solvent in the course of several days afforded abundant colorless crystals of **2**. X-ray quality crystals were obtained at −30 °C. They were coated with a protective oil prior to structure determination. For other characterization purposes and to remove excess of oily $As(SiMe_3)_3$, the crystalline solid was briefly washed with cold hexane and evacuated for a few minutes. Melting point: 68–70 °C, clear liquid. Anal. Found (calcd) for $C_9H_{29}NAlAsSi_2$: C, 34.62 (34.94); H, 9.28 (9.45); N, 4.29 (4.53). ^1H NMR (toluene-d_8/benzene-d_6): δ 0.56/0.61 (18H; $SiMe_3$), 2.01/1.85 (9H, NMe_3), 4.0/4.0 (2H, very broad; AlH_2). $^{13}C\{^1H\}$ NMR (toluene-d_8) (intensity; assignment): δ 5.2 (70; $SiMe_3$); 47.3 (100; NMe_3). MS: m/e (intensity) (ion): peak clusters around: 309 (8) ($[H_2AlAs(SiMe_3)_2] \cdot NMe_3$ or M), 294 (100) (M − Me or $As(SiMe_3)_3$), 279 (16) (M − 2Me or $As(SiMe_3)_3$) − Me), 250 (2) (M − NMe_3), 222 (40) ($HAs(SiMe_3)_2$), 206 (43) (M − NMe_3 − 3Me + H), 191 (7) (M − NMe_3 − 4Me + H), 177 (3) (M − NMe_3 − $SiMe_3$), 147 (6) (M − NMe_3 − $SiMe_3$ − 2Me), 134 (6) ($SiAsAlH_4$), 73 (63) ($SiMe_3$), 59 (8) ($HSiMe_2$). IR: ν(Al−H) 1784 cm^{-1}. Note, the insoluble decomposition product of **2** that was

8

obtained from the reaction mixture upon long storage showed by IR spectrometry a broad stretch ν(Al–H) at 1795 cm^{-1}.

(2) Thermal decomposition. A sample of **2**, 0.71 g or 2.3 mmol, was pyrolyzed in a sublimer for two hours at 450 °C under vacuum, and with the collection of volatiles. Small quantities of a colorless, oily liquid, likely As(SiMe$_3$)$_3$, distilled out. Additionally, after completion of pyrolysis, some colored solids were found on the colder parts of the set-up. The solid pyrolysis product was a dark gray/black solid, 0.25 g or weight loss 65%. Noncondensables (CH$_4$ and H$_2$), 1.5 mmol; condensables (HSiMe$_3$ and NMe$_3$), 5.1 mmol; weight of volatiles, approximately 0.3 to 0.4 g. A XRD pattern for the black product showed very broad peaks consistent with the onset of AlAs crystallinity; average particle size, approximately 2 nm. EA for the black product: Al, 37.96; As, 59.18; C, 0.38; H, 0.67; Si (by difference), 1.81; Al/As = 1.78.

Structural determinations for 1 and 2.

Specimens of **1** and **2** were stored at −30° C prior to determinations. The intensity data were collected on a Siemens SMART diffractometer using the omega scan mode. For **1**, systematic absences and diffraction symmetry indicated the trigonal space group P–3; cell dimensions were obtained from 5558 reflections with 2Θ 3.00–50.00°. For **2**, the data determined the monoclinic space group P2$_1$; cell dimensions were obtained from 6832 reflections with 2Θ 3.00–50.00°. The structures were solved by direct methods. All non-hydrogen atoms were refined with anisotropic displacement parameters. All hydrogen atoms, including Al-hydrogens, were placed in ideal positions and refined as riding atoms with relative isotropic displacement parameters. The Al–H bond length was assumed at 1.50 Å. Details of the data collection for **1** and **2** are summarized in Table 1, and Table 2 shows selected bond distances and angles.

9

Results and Discussion

The combination of $H_3Al \cdot NMe_3$ and $P(SiMe_3)_3$ in diethyl ether at ambient conditions resulted in a high yield of the dehydrosilylation product, trimer $[H_2AlP(SiMe_3)_2]_3$ (**1**), as described in equation 1.

$$H_3Al \cdot NMe_3 + P(SiMe_3)_3 \xrightarrow{\text{Et}_2\text{O}} 1/3[H_2AlP(SiMe_3)_2]_3 + HSiMe_3 + NMe_3 \qquad (1)$$

Such an outcome was expected based on the trimeric nature of products from other related systems such as $H_3Ga/E(SiMe_3)_3$, $E = P$, As,[2c] and $H_3B \cdot THF/P(SiMe_3)_3$.[1a] On the other hand, a reaction between $H_3Al \cdot NMe_3$ and $As(SiMe_3)_3$ under comparable conditions yielded a different dehydrosilylation product, base-stabilized monomer $[H_2AlAs(SiMe_3)_2] \cdot NMe_3$ (**2**), according to the following equation.

$$H_3Al \cdot NMe_3 + As(SiMe_3)_3 \xrightarrow{\text{Et}_2\text{O}} [H_2AlAs(SiMe_3)_2] \cdot NMe_3 + HSiMe_3 \qquad (2)$$
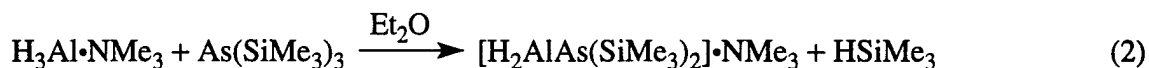
Interestingly, two related P and As derivatives $[H_2AlEMes_2] \cdot NMe_3$, $E = P$, As,[5] were both base-stabilized adducts. Although it is tempting in these cases to speculate on the significance of such intrinsic bonding factors as bond strength and/or steric influence, it may simply be that variations in reaction conditions are responsible for the nature of the isolated product, i.e., oligomer or base-stabilized adduct. We note that for $E = P$ there was a NMR evidence for a minor byproduct containing a coordinated NMe_3 molecule and this could be a transient or coexisting with **1** based-stabilized $[H_2AlP(SiMe_3)_2] \cdot NMe_3$. In this regard, the related $[H_2AlPMes_2] \cdot NMe_3$ was reported to lose NMe_3 when heated under vacuum and convert to the proposed species of empirical formula $[H_2AlPMes_2]_n$. We, too, noticed a similar effect for $[H_2AlAs(SiMe_3)_2] \cdot NMe_3$ upon its prolonged evacuation at

10

ambient conditions; however, an accompanying decomposition associated with the formation of As(SiMe$_3$)$_3$ prevented us from isolation of well defined byproduct(s). In yet another relevant report, heating [H$_2$AlN(SiMe$_3$)$_2$]·NMe$_3$[4a,b] appeared to result in disproportionation chemistry rather than simple removal of the coordinated amine. Finally, no reaction was detected in this study between H$_3$Al·NMe$_3$ and N(SiMe$_3$)$_3$ even after reflux in Et$_2$O in accord with a rather notorious lack of reactivity of this amine toward HSiMe$_3$ elimination, as reported earlier from this laboratory.[2] It is interesting to note, however, that N(SiMe$_3$)$_3$ underwent Me$_3$SiCl elimination reactions with haloboranes.[11]

Trimer **1** appeared to be quite stable at room temperature, at least after isolation and in toluene solutions. Under these conditions, it was decomposing slowly with the formation of free P(SiMe$_3$)$_3$ and HSiMe$_3$. For example, by NMR spectroscopy, after 3 weeks approximately 25% of it had decayed. Under comparable conditions, the NMR toluene-d$_8$ solution of **2** was barely decomposed after 2 weeks with only traces of HSiMe$_3$ and possible As(SiMe$_3$)$_3$ formed. This kind of stability of isolated **2** was somewhat surprising since if **2** was left in the mother liquor it would have turned rather fast to an insoluble solid. Generally, pnictinoalane derivatives **1** and **2** showed higher stabilities than the related pnictinogallane trimers [H$_2$GaE(SiMe$_3$)$_2$]$_3$, E = P, As;[2c] in the latter cases, the evolution of dihydrogen was additionally observed due to the higher thermal frailty of the Ga–H bond.

The elemental analysis for compound **1** was consistent with the stoichiometry of {H$_2$AlP(SiMe$_3$)$_2$}. Such a make-up was supported also by the ^{1}H NMR resonance at δ 4.4, in the range expected for protons in the AlH$_2$ groups. The presence of such groups in **1** was further corroborated by its IR spectrum displaying an Al–H stretching band at 1796 cm^{-1}. The remaining NMR data for the compound were of somewhat limited value in elucidating structural features. Both ^{1}H and ^{13}C{^{1}H} NMR spectra showed regularly spaced four-line multiplets for protons and carbons in the SiMe$_3$ groups, respectively, suggesting a complex structure in solution. This information however excluded a planar

dimer where virtual triplets would have been expected. Interestingly, the ^{1}H NMR spectrum for the closely related gallium derivative [H$_2$GaP(SiMe$_3$)$_2$]$_3$ displayed a broadened doublet for the SiMe$_3$ protons.[2c] Strong support for the trimeric species in the gaseous state was provided by mass spectrometry. The spectrum contained the molecular ion for the species {[H$_2$AlP(SiMe$_3$)$_2$]$_3$ − H} as the highest m/e cluster and other logical fragments.

The elemental analysis for compound **2** supported its formulation as the monomeric base-stabilized adduct [H$_2$AlAs(SiMe$_3$)$_2$]·NMe$_3$. The presence of the coordinated NMe$_3$ in **2** was substantiated by the ^{1}H and ^{13}C{^{1}H} NMR spectra in toluene-d$_8$ which showed the resonances at δ 2.01 and 47.3, respectively, for the amine. The ^{1}H NMR spectrum contained also a singlet in the SiMe$_3$ region and an extremely broad signal at approximately δ 4.0. The latter resonance was consistent with the presence of the AlH$_2$ moiety as was the infrared Al−H stretching band observed at 1784 cm^{-1}. Further corroboration of the structure was provided by mass spectrum for **2** which showed the expected molecular ion at m/e 309.

The solid state structures of compounds **1** and **2** were authenticated by single-crystal X-ray structure determinations. Figure 1 shows the thermal ellipsoid diagram for compound **1**. The structure is solved as a planar six-membered ring of alternating four-coordinated Al and P atoms. Its major features, although interesting, are not novel in that they match those found in three other related trimers, [H$_2$GaE(SiMe$_3$)$_2$]$_3$ (E = P, As),[2c] and [H$_2$BP(SiMe$_3$)$_2$]$_3$.[1a] For example, the thermal parameters for the Al atom in **1** are about twice the magnitude of the P atom, in accord with the trend in this family of compounds. As mentioned earlier, this may be indicative of the molecular symmetry of **1** being lower than the crystallographic site symmetry and the ring probably not planar. Similarly, the ring Al−P−Al angle, 126.42(7)°, is larger the corresponding P−Al−P angle, 113.58(8)°, which is also true for the respective angles at group 13 and 15 atoms in the related compounds. The Al−P bond length, av 2.398 Å, is reportedly one of the shortest

for four-coordinated Al and P compounds. Comparable Al–P distances are found in the mixed-metal, P-bridged, four-membered ring $(Et_2O)_2Li[\mu\text{-}P(SiMe_3)_2]_2AlH_2$,[2b] 2.4001(13) Å, in the monomeric base-stabilized adduct $[H_2AlPMes_2]\cdot NMe_3$,[5] 2.409(3) Å, and in the aluminaphosphacubane $[i\text{-}BuAl(\mu_3\text{-}PSiPh_3)]_4$,[12a] 2.414(4) Å. In sterically crowded derivatives of $\{(Me_3Si)_3Al\}$ somewhat longer Al–P bond lengths are reported for the dimers $[(Me_3Si)_2AlPPh_2]_2$, 2.446(4) Å, and $[(Me_3Si)_2AlP(SiMe_3)Ph]_2$, 2.466(2) Å, and trimer $[(Me_3Si)_2AlP(H)(c\text{-}C_6H_{11})]_3$, 2.444(4) Å.[1c] A similar Al–P bond length range is observed for the dimers $[Et_2AlP(SiMe_3)_2]_2$,[12b] 2.460(1) Å, $[Me_2AlP(SiMe_3)_2]_2$,[12c] 2.460(1) Å, $[Bu^i_2AlP(SiMe_3)_2]_2$,[12d] 2.469(2) Å, the six-membered ring compounds $[Me_2AlCH_2PMe_2]_2$,[12e] 2.451(2) Å, and $[ClAl(CH_2PMe_2)_2]_2$,[12e] 2.425(1) Å, and in the gas phase for the trimer $[Me_2AlPMe_2]_3$,[12f] 2.434(4) Å. On the other hand, in the complex cage structure of $[P_4(Cp^*Al)_6]$ the Al–P distances for the four-coordinated P atoms average at 2.406 Å while for the tri-coordinated P atoms at 2.327 Å; further, in the zinc blende structure of AlP this distance has the value of 2.35 Å.[13] It is instructive to compare all these bond lengths with the recently published *ab initio* calculations of the structures of the dimer $[H_2AlPH_2]_2$ and cubic cluster $[HAlPH]_4$ that provided the Al–P distances of 2.451 Å and 2.434 Å, respectively.[14]

The structure of the monomeric base-stabilized adduct $[H_2AlAs(SiMe_3)_2]\cdot NMe_3$ (**2**) is one of the rare authenticated aluminum-arsenic compounds and is the first reported for the parent AlH_2-containing alane arsenide. The characteristic feature of this structure is that it contains four-coordinated aluminum bonded to three-coordinated arsenic. This could partially explain the fact that the Al–As bond length in **2**, 2.4383(21) Å, is very short and, actually, is the shortest bond of this type reported to date. For example, in the mixed-metal, As-bridged, four membered-ring $(Et_2O)_2Li[\mu\text{-}As(SiMe_3)_2]_2AlH_2$ this distance is at 2.4934(7) Å.[2b] Distances longer than that are found in the dimers $[Et_2AlAs(t\text{-}Bu)_2]_2$,[15a] av 2.567 Å, $[Et_2AlAs(SiMe_3)_2]_2$,[15b] av 2.535 Å, and trimers $[Me_2AlAsPh_2]_3\cdot(C_7H_8)_2$,[15c] av 2.524 Å, $[Me_2AlAs(CH_2SiMe_3)Ph]_3$,[15c] av 2.518 Å ($2.504(5)$ Å$_{min}$–$2.526(5)$ Å$_{max}$).

We note that in two other reported similar structures of the monomeric base-stabilized adducts, [H(Cl)AlN(SiMe₃)₂]•NMe₃[1c] and [H₂AlPMes₂]•NMe₃,[5] relatively very short Al–pnictide covalent distances are also observed. In addition to the very short Al–As distance in **2**, the dative bond length between Al and N from coordinated NMe₃, 1.998(7) Å, requires special attention. This length appears to be among the shortest for alane trimethylamine adducts. This is illustrated by the relevant dative Al–N lengths in the compounds [H₂AlPMes₂]•NMe₃,[5] 2.009(8) Å and [H(Cl)AlN(SiMe₃)₂]•NMe₃,[1c] 2.016(5) Å, and in simple adducts such as (Me₃Si)₃Al•NMe₃,[4b] 2.040(6) Å and [(Me₃Si)₃Al]₂TMEDA,[16a] 2.069(5) Å. This bond is also shorter than the Al–N distances in the monomeric H₃Al•NMe₃ (gas phase),[16b] 2.063(8) Å and monomeric Me₃Al•NMe₃ (gas phase),[16c] 2.099(10) Å. Apparently, the large effective Lewis acidity of Al in the monomeric unit [H₂AlAs(SiMe₃)₂] of **2** is more efficiently fulfilled through interaction with the lone electron pair on nitrogen in NMe₃ than with the available electron pair on the neighboring arsenic. The presence of the latter electron pair can be inferred from the pyramidal configuration of ligands around arsenic (sum of angles, 298.1°).

In the first approximation, compounds **1** and **2** seem to be good precursors for pyrolytic conversion to AlP and AlAs, respectively, *via* dehydrosilylation. In the case of **2**, the conversion would additionally require that the coordinated NMe₃ is efficiently removed without significantly influencing the target elimination chemistry. We note, however, that our observations concerning the compounds' stabilities indicate that, in addition to HSiMe₃ elimination, thermally enhanced ligand redistribution may take place resulting in the formation of E(SiMe₃)₃ and therefore altering the nature of products. Additionally, although not observed in this study at ambient conditions, reductive decomposition with the evolution of dihydrogen and formation of elemental aluminum, a common decomposition pathway for alanes,[17] may become significant at higher temperatures as well. For example, regarding the latter aspect, one of the compounds discussed above, [H₂AlPMes₂]•NMe₃, was reported as an OMCVD source to deposit

14

aluminum films.[5] Such a decomposition pathway above, however, could be due to likely higher energy barriers of mesitylene formation under specific CVD conditions than trimethylsilane formation in our bulk decomposition. In order to assess the feasibility of the conversion of **1** and **2** to AlP and AlAs, respectively, exploratory pyrolysis experiments were carried out.

The pyrolysis of **1** was performed at 450 and 950 °C under vacuum. The experiment at 450 °C was done with collection and analysis of volatiles. The volatiles consisted of $HSiMe_3$, CH_4, and H_2; small amounts of an oily colorless liquid, likely $P(SiMe_3)_3$, were also observed to distill out. The presence of $HSiMe_3$ was expected from the target dehydrosilylation chemistry but the remaining compounds pointed out also to other decomposition pathways. In regard to that, methane and hydrogen were commonly observed during pyrolysis of $SiMe_3$-containing precursors although significant quantities of the latter were observed at still higher temperatures,[1b, 2c, 18] and hydrogen could additionally be formed *via* reductive decomposition of the AlH_2 groups. The brown solid product from this experiment showed by XRD spectroscopy the onset of AlP crystallinity. On the other hand, the pyrolysis at 950 °C afforded a black solid that was shown to contain the nanocrystalline cubic AlP with 5 nm average crystallite size. The elemental analysis yielded Al/P ratio 1, consistent with the AlP stoichiometry, but also significant proportions of residual Si and C. Based on these observations, we concluded that the formation of AlP from dehydrosilylation was accompanied by side-decomposition of residual $SiMe_3$ and AlH_2 (likely) groups. Also, compound **1** (or derived byproducts) must have volatilized significantly during both pyrolyses because we observed a side-effect formation of uniform, very robust, golden-like thin films on the entire surface of the pyrolysis tube.

The pyrolysis of **2** was performed at 450 °C under vacuum with the collection and analysis of volatiles, similarly as above. $HSiMe_3$, NMe_3, CH_4, and H_2 were detected in the volatiles and significant quantities of condensed liquid, likely $As(SiMe_3)_3$, were observed on the cold parts of the set-up as well. The condensable volatiles contained, in

15

addition to HSiMe$_3$, some NMe$_3$ which we were able to identify by IR spectroscopy but unable to separate from HSiMe$_3$ and quantify due to the closeness of their vapor pressures. The black solid product was shown by XRD to contain nanocrystalline cubic AlAs with an average crystallite size of approximately 2 nm. The lack of nitrogen in the elemental analysis of the solid was consistent with an efficient removal of the amine while relatively low Si and C contents indicated a rather small-sized side-decomposition of residual SiMe$_3$ groups. The Al/As ratio of 1.78 indicated, however, significant excess of aluminum (possibly in the form of elemental Al) $vs.$ the expected ratio 1 for AlAs. This piece of data could be linked to the formation of removable As(SiMe$_3$)$_3$ and therefore depletion in arsenic of the solid product, and was likely associated with the specific decomposition pathway for alanes and gallanes, namely, reductive coupling with H$_2$ evolution and metal formation. We point out that similar composition characteristics were previously observed in the pyrolysis of the related gallane derivative, i.e., the polymeric solid derived from unstable [H$_2$GaAs(SiMe$_3$)$_2$]$_3$, which yielded a product containing nanocrystalline GaAs and showing Ga/As ratio 1.5.[2c] In summary, our preliminary pyrolysis experiments for **1** and **2** demonstrated that these precursors were subject to dehydrosilylation and could be pyrolyzed toward nanocrystalline AlP and AlAs, respectively. However, under the applied pyrolysis conditions, other decomposition pathways competed in these systems and contributed to retention of residuals containing Si and C, most likely in the form of separate (to the crystalline product) amorphous phases. In the case of **2**, the intrinsic decomposition pathway for alanes, reductive coupling, appeared to be especially pronounced and afforded the aluminum enriched product.

Supporting Information: Information on collection of data and refinement, crystal packing diagrams, tables of bond distances, bond and torsion angles, anisotropic temperature factor parameters, and atomic fractional coordinates for **1** and **2** (12 pages). Ordering information is given on any current masthead page.

References

(1) For example, see: (a) Wood, G. L.; Dou, D.; Narula, C. K.; Duesler, E. N.; Paine, R. T.; Nöth, H. *Chem. Ber.* **1990**, *123*, 1455 and references therein. (b) Janik, J. F.; Duesler, E. N.; Paine, R. T. *Inorg. Chem.* **1987**, *26*, 4341. (c) Janik, J. F.; Duesler, E. N.; McNamara, W. F.; Westerhausen, M; Paine, R. T. *Organometallics* **1989**, *8*, 506.

(2) (a) Janik, J. F.; Wells, R. L.; Young, V. G., Jr., Halfen, J. A. *Organometallics* **1997**, *16*, 3022. (b) Janik, J. F.; Wells, R. L.; White, P. S. *Organometallics* **1998**, submitted for publication. (c) Janik, J. F.; Wells, R. L.; Young, V. G., Jr.; Rheingold, A. L.; Guzei, I. A. *J. Am. Chem. Soc.* **1998**, *120*, 532.

(3) (a) Elms, F. M.; Koutsantonis, G. A.; Raston, C. L. *J. Chem. Soc., Chem. Commun.* **1995**, 1669. (b) Cowley, A. H.; Harris, P. R.; Jones, R. A.; Nunn, C. M. *Organometallics* **1991**, *10*, 652.

(4) (a) Janik, J. F.; Paine, R. T. *XVth Int. Conference on Organometallic Chemistry*, Warsaw, Poland, August 1992, P113. (b) Janik, J. F.; Duesler, E. N.; Paine, R. T. *J. Organomet. Chem.* **1997**, *539*, 19. (c) Gardiner, M.; Koutsantonis, G. A.; Lawrence, S. M.; Lee, F.-C.; Raston, C. L. *Chem. Ber.* **1996**, *129*, 545.

(5) Atwood, D. A.; Contreras, L.; Cowley, A. H.; Jones, R. A.; Mardones, M. A. *Organometallics* **1993**, *12*, 17.

(6) Shriver, D. F.; Drezdzon, M. A. *"The Manipulation of Air Sensitive Compounds"*, Wiley-Interscience, New York, 1986.

18

(7) Kovar, R. A.; Callaway, J. O. *Inorg. Synth.* **1977**, *17*, 36.

(8) Becker, G.; Hölderich, W. *Chem. Ber.* **1975**, *108*, 2484.

(9) (a) Becker, G.; Gutenkunst, G.; Wessely, H. J. *Z. Anorg. Allg. Chem.* **1980**, *462*, 113. (b) Wells, R. L.; Self, M. S.; Johansen, J. D.; Laske, J. A.; Aubuchon, S. R.; Jones, L. J. *Inorg. Synth.* **1997**, *31*, 150.

(10) Gabe, E. J.; Le Page, Y.; Charland, J.-P.; Lee, F. L.; White, P. S. *J. Appl. Cryst.* **1989**, *22*, 384.

(11) For example, see: (a) Janik, J. F.; Narula, C. K.; Gulliver, E. G.; Duesler, E. N.; Paine, R. T. *Inorg. Chem.* **1988**, *27*, 1222. (b) Barlos, K.; Christl, H.; Nöth, H. *Liebigs Ann. Chem.* **1976**, 2272. (c) Srivastava, G. *J. Organomet. Chem.* **1974**, *69*, 179.

(12) (a) Cowley, A. H.; Jones, R. A.; Mardones, M. A.; Atwood, J. L.; Bott, S. G. *Angew. Chem. Int. Ed. Engl.* **1990**, *29*, 1409. (b) Wells, R. L.; McPhail, A. T.; Self, M. F.; Laske, J. A. *Organometallics* **1993**, *12*, 3333. (c) Hey-Hawkins, E.; Lappert, M. F.; Atwood, J. L.; Bott, S. G. *J. Chem. Soc. Dalton Trans.* **1991**, 939. (d) Krannich, L. K.; Watkins, C. L.; Schauer, S. J.; Lake, C. H. *Organometallics* **1996**, *15*, 3980. (e) Karsch, H. H.; Appelt, A.; Köhler, F. H.; Müller, G. *Organometallics* **1985**, *4*, 231. (f) Haaland, A.; Hougen, J.; Volden, H. V.; Hanika, G. H.; Karsch, H. H. *J. Organomet. Chem.* **1987**, *322*, C24.

(13) Dohmeier, C.; Schnöckel, H.; Robl, C.; Schneider, U.; Ahlrichs, R. *Angew. Chem. Int. Ed. Engl.* **1994**, *33*, 199.

(14) Davy, R. D.; Schaefer, H. F., III *J. Phys. Chem. A* **1997**, *101*, 5707.

(15) (a) Heaton, D. E.; Jones, R. A.; Kidd, K. B.; Cowley, A. H.; Nunn, C. M. *Polyhedron* **1988**, *7*, 1901.   (b) Wells, R. L.; McPhail, A. T.; Speer, T. M.; *Organometallics* **1992**, *11*, 960.   (c) Laske-Cooke, J. A.; Purdy, A. P.; Wells, R. L.; White, P. S. *Organometallics* **1996**, *15*, 84.

(16) (a) Goebel, D. W.; Hencker, J. L.; Oliver, J. P. *Organometallics*, **1983**, *2*, 746. (b) Almenningen, A.; Gundersen, G.; Haugen, T.; Haaland, A. *Acta Chem. Scand.* **1972**, *26*, 3928. (c) Anderson, G. A.; Almenningen, A.; Forgaard, F. R.; Haaland, A. *J. Chem. Soc., Chem. Commun.* **1971**, 480.

(17) For example, see review: Jones, C.; Koutsantonis, G. A.; Raston, C. L. *Polyhedron* **1993**, *12*, 1829.

(18) Janik, J. F.; Baldwin, R. A.; Wells, R. L.; Pennington, W. T.; Schimek, G. L.; Rheingold, A. L.; Liable-Sands, L. M. *Organometallics* **1996**, *15*, 5385.

Table 1. Crystallographic Data and Measurements for **1** and **2**.

	1	**2**
molecular formula	$C_{18}H_{60}Al_3P_3Si_6$	$C_9H_{29}AlAsSi_2N$
formula weight	619.05	309.41
crystal system	trigonal	monoclinic
space group	$P-3$	$P2_1$
a, Å	11.8152(7)	9.1285(5)
b, Å		11.1657(6)
c, Å	16.7019(10)	9.1283(6)
β, deg		104.274(1)
V, Å^3	2019.20(17)	901.69(9)
Z	2	2
μ, mm^{-1}	0.40	2.04
temp, K	223(2)	173(2)
D_{calcd}, g/cm^3	1.018	1.140
crystal dimensions, mm	0.25 x 0.25 x 0.15	0.20 x 0.20 x 0.35
Θ range for data collection (deg)	1.50-25.00	1.50-25.00
no. of rflns collected	17793	7955
no. of unique rflns	2417	3173
no. of rflns (I > 2.5σ(I))	1916	2823
R (I > 2.5σ(I));[a] R_w[b]	0.066; 0.079	0.048; 0.057
R (all data);[a] R_w[b]	0.101; 0.105	0.054; 0.060
goodness-of-fit[c]	4.46	2.44
final max/min $\Delta\rho$, e/Å^{-3}	0.390/−0.400	1.45/−0.820

[a] $R = \Sigma||F_o| - |F_c||/\Sigma|F_o|$; [b] $R_w = [\Sigma w(|F_o| - |F_c|)^2/\Sigma w|F_o|^2]^{1/2}$

[c] $GooF = [\Sigma[w(|F_o| - |F_c|)^2]/(n - p)]^{1/2}$

Table 2. Selected Bond Distances (Å) and Angles (°) for **1** and **2** with Estimated Standard Deviations in Parentheses

	Bond Lengths		
1		**2**	
P(1)–Al(1)	2.3916(16)	As(1)–Al(1)	2.4383(21)
P(1a)–Al(1)	2.4041(14)	Al(1)–N(1)	1.998(7)
P–Si (av)	2.263	As–Si (av)	2.344
Si–C (av)	1.840	Si–C (av)	1.865
Si–C; min/max	1.832(8)/1.849(8)	Si–C; min/max	1.850(9)/1.883(7)

	Bond Angles		
1		**2**	
P(1)–Al(1)–P(1a)	113.58(8)	As(1)–Al(1)–N(1)	105.90(19)
Al(1)–P(1)–Al(1b)	126.42(7)	Si(1)–As(1)–Si(2)	104.82(7)
Si(1)–P(1)–Si(2)	107.83(8)	Al–N–C (av)	109.8
Al–P–Si (av)	105.4	Al–As–Si (av)	96.7
P–Al–H (av)	108.4	As–Si–C (av)	110.4

	Torsion Angles		
1		**2**	
Al(1)–P(1)–Si(1)–C(13)	173.5(6)	Si(1)–As(1)–Al(1)–N(1)	−127.2(3)
Al(1)–P(1)–Si(2)–C(23)	−173.4(6)	Si(2)–As(2)–Al(1)–N(1)	126.9(3)
Al(1)–P(1)–Si(2)–C(22)	65.9(4)	As(1)–Al(1)–N(1)–C(2)	179.8(8)

Captions for Figures

Figure 1. Thermal ellipsoid diagram (35% probability ellipsoids) showing the molecular structure of **1**. All carbon-hydrogen atoms are omitted for clarity.

Figure 2. Thermal ellipsoid diagram (35% probability ellipsoids) showing the molecular structure of **2**. All carbon-hydrogen atoms are omitted for clarity.

C21

C12

C23

C13

Si2

C22

Si1

C11

P1

Al1
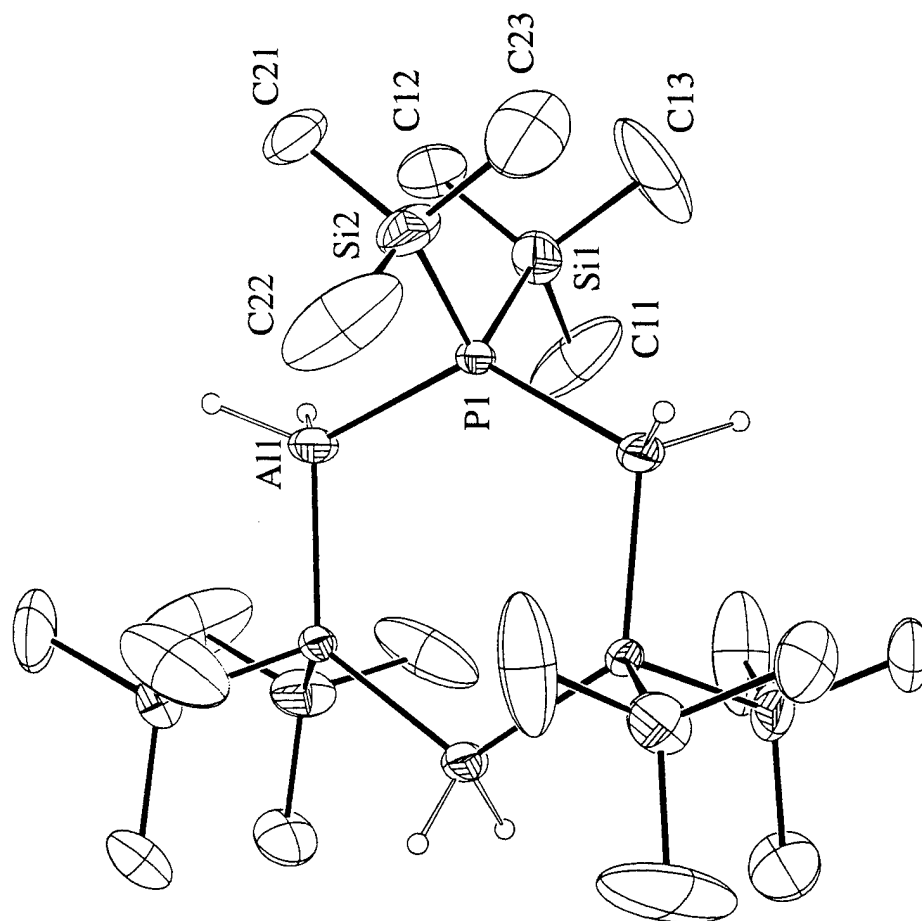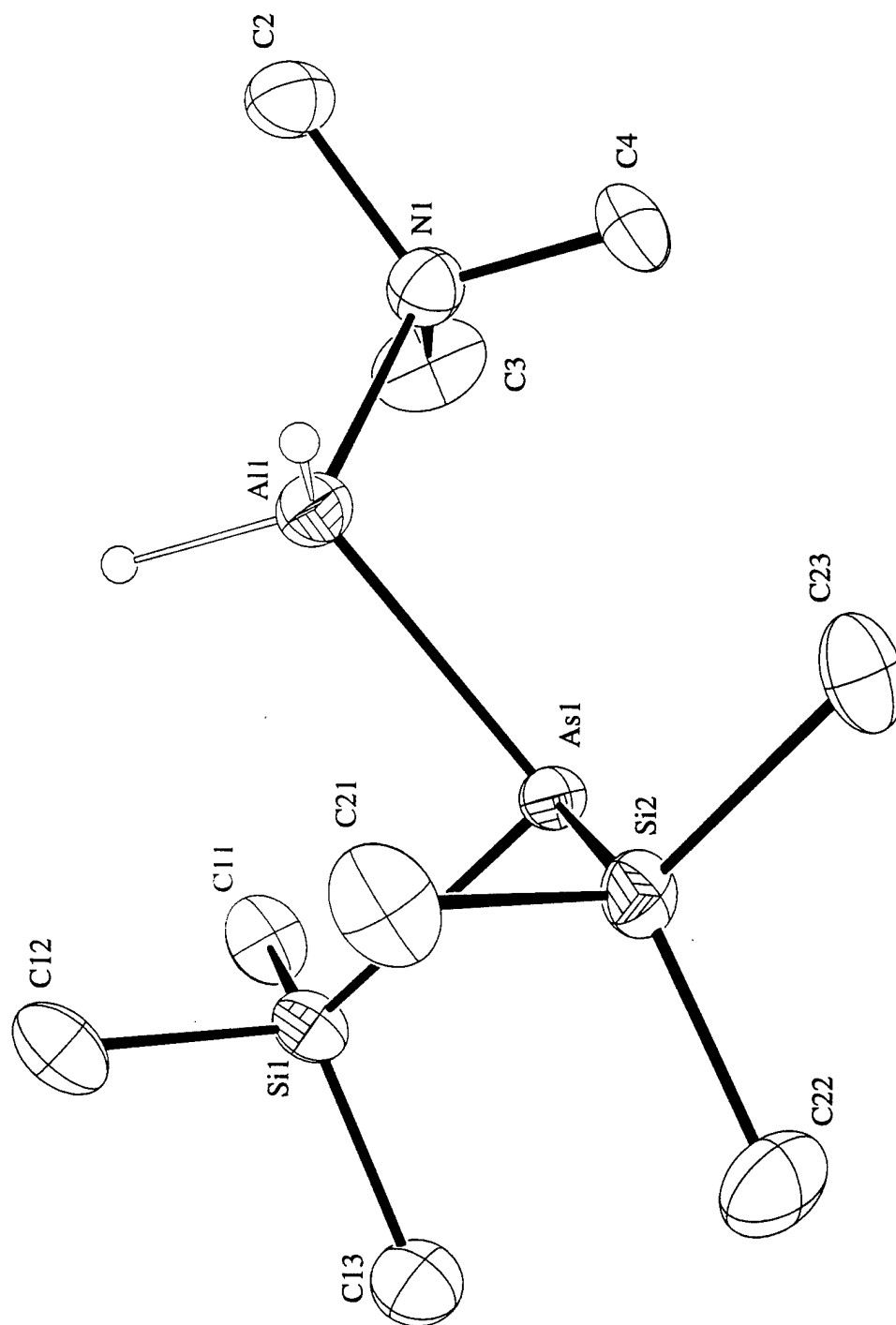
TECHNICAL REPORTS DISTRIBUTION LIST

ORGANOMETALLIC CHEMISTRY FOR ELECTRONIC & OPTICAL MATERIALS

Dr. Harold E. Guard
Code 1113
Chemistry Division, 331
Office of Naval Research
800 N. Quincy Street
Arlington, VA 22217-5660

Defense Technical Information
  Center (DTIC)
Ft. Belvoir Headquarters Complex
8725 John J. Kingman Road
STE 0944
Ft. Belvoir, VA 22060

Dr. James S. Murday
Chemistry Division, Code 6100
Naval Research Laboratory
Washington, DC 20375-5320

Dr. John Fischer, Director
Chemistry Division, C0235
Naval Naval Air Weapons Center
  Weapons Division
China Lake, CA 93555-6001

Dr. Richard W. Drisko
Naval Facilities & Engineering
  Service Center
Code L52
Port Hueneme, CA 93043

Dr. Eugene C. Fischer
Code 2840
Naval Surface Warfare Center
  Carderock Division Detachment
Annapolis, MD 21402-1198

Dr. Bernard E. Douda
Crane Division
Naval Surface Warfare Center
Crane, IN 47522-5000

Dr. Peter Seligman
Naval Command, Control and
  Ocean Surveillance Center
RDT&E Division
San Diego, CA 93152-5000